Oligomeric and Subunit Structure of the *Helicobacter Pylori* Vacuolating Cytotoxin

Pietro Lupetti,* John E. Heuser,‡ Roberto Manetti,§ Paola Massari,§ Salvatore Lanzavecchia,‖ Pier Luigi Bellon,‖ Romano Dallai,* Rino Rappuoli,§ and John L. Telford§

*Dipartimento di Biologia Evolutiva, Università di Siena, 53100 Siena, Italy; ‡Department of Cell Biology and Physiology, Washington University School of Medicine, St. Louis, Missouri 63110-1093; §IRIS, The Chiron Biocine Immunobiological Research Institute, 53100 Siena, Italy; and ‖Dipartimento di Chimica Strutturale e Stereochimica Inorganica, Università di Milano, 20133 Milano, Italy

Abstract. Disease-associated strains of *Helicobacter pylori* produce a potent toxin that is believed to play a key role in peptic ulcer disease in man. In vitro the toxin causes severe vacuolar degeneration in target cells and has thus been termed VacA (for vacuolating cytotoxin A). Cytotoxic activity is associated with a >600-kD protein consisting of several copies of a 95-kD polypeptide that undergoes specific proteolytic cleavage after release from the bacteria to produce 37- and 58-kD fragments. Quick freeze, deep etch electron microscopy has revealed that the native cytotoxin is formed as regular oligomers with either six- or sevenfold radial symmetry. Within each monomer, two domains can clearly be distinguished, suggesting that the 37- and 58-kD fragments derive from proteolytic cleavage between discrete subunits of the monomer. Analysis of preparations of the toxin that had undergone extensive cleavage into the 37- and 58-kD subunits supports this interpretation and reveals that after cleavage the subunits remain associated in the oligomeric structure. The data suggest a structural similarity with AB-type toxins.

MANY bacterial protein toxins that interact with cell membranes form high molecular weight oligomers. In some cases, such as the hemolysins, cytotoxicity is due to the formation of aqueous channels by insertion of the oligomers into the cell membrane (Harris et al., 1991; Bahkdi and Tranum-Jensen, 1991; Ballard et al., 1993; Bahkdi et al., 1985; Sekiya et al., 1993; van der Goot et al., 1992). Others, whose cytotoxicity is due to enzymatic modification of intracellular substrates, are composed of two distinct moieties (A+B). The active (A) moiety possesses the enzymatic activity whereas the oligomeric binding (B) moiety is required for target cell interaction and translocation of the A moiety across the plasma membrane. Interestingly, the B moieties of several of these toxins insert into membranes to form ion-conductive channels (Milne et al., 1994; Hoch et al., 1985). B moieties may vary from the anthrax toxin protective antigen (Leppla, 1995), which forms membrane active heptamers at acid pH (Milne et al., 1994), to the homo- and heteropentameric B moieties of cholera toxin and pertussis toxin (Domenighini et al., 1995), which are assembled in the periplasm before release from the bacteria. Here we describe structural properties of a novel unrelated toxin from *Helicobacter pylori* that extend our knowledge of the variety of oligomeric structures that bacterial toxins can form.

The *H. pylori* vacuolating cytotoxin (VacA)[1] is a soluble protein that is released from type I strains of the bacteria (Cover and Blaser, 1992*a*; Xiang et al., 1995). The toxin is believed to play a key role in disease induced by *H. pylori* infection (Telford et al., 1994*b*; Xiang et al., 1995), which is the major cause of peptic ulcer in man (Cover and Blaser, 1992*b*) and is tightly associated with gastric cancer (Parsonnet, 1993). Highly purified cytotoxin causes gastric epithelium necrosis and ulceration when administered orally to mice (Telford et al., 1994*b*). Furthermore, in a recently developed mouse model of *H. pylori* infection, cytotoxic strains caused severe gastritis and ulceration similar to the pathology observed in severe disease in man, whereas noncytotoxic strains caused only mild gastritis (Marchetti et al., 1995). In this model, oral immunization with highly purified cytotoxin conferred protection against infection by cytotoxic strains of *H. pylori* and is thus a major candidate for inclusion in an anti–*H. pylori* vaccine.

In vitro the cytotoxin causes massive vacuolation and death in a number of human cell lines of diverse origin (Leunk, 1991). The vacuoles induced are acidic and derive from the fluid-phase endocytic pathway as evidenced by the accumulation of lucifer yellow dye. Furthermore, the vacuoles can be stained with antibodies against the vacuolar V-ATPase (Papini et al., 1995) and the rab7 small GTP-

Address all correspondence to John L. Telford, IRIS, Via Fiorentina 1, 53100 Siena, Italy. Tel.: 39-577-343470. Fax: 39-577-243564.

1. *Abbreviation used in this paper*: VacA, *Helicobacter pylori* vacuolating cytotoxin.

binding protein (Papini et al., 1994) that associates specifically with the late endosome compartment of the endocytic pathway (Zerial and Stenmark, 1993), suggesting that the toxin may interfere at this stage in endosome trafficking (Papini et al., 1994; Telford et al., 1994*a*).

The *vacA* gene codes for a 140-kD precursor protein that is processed during export from the bacteria by carboxy-terminal cleavage to produce a 95-kD polypeptide (Telford et al., 1994*b*; Cover et al., 1994; Schmitt and Haas, 1994). Similarities have been noted between the carboxy-terminal 45 kD of the precursor polypeptide and the carboxy-terminal region of the IgA protease family of exotoxins (Schmitt and Haas, 1994). This region of the IgA protease precursor is involved in outer membrane transport, suggesting that the 95-kD polypeptide may be exported in a similar fashion. After release from the bacteria, the 95-kD VacA polypeptide undergoes specific proteolytic cleavage at a short repeated sequence of eight amino acids to produce a 37-kD amino-terminal fragment and a 58-kD carboxy-terminal fragment that copurify on gel filtration, indicating that they remain associated after cleavage (Telford et al., 1994*b*). The relevance of this further processing to toxic activity is not yet clear; however, it suggests that the protein may be structured in two distinct subunits.

Purification of cytotoxic activity from *H. pylori* culture supernatants revealed that the toxin is a large oligomeric protein that migrates in gel filtration at an apparent molecular mass of >600 kD (Cover and Blaser, 1992*a*). This high molecular weight oligomeric material very effectively induced high titre neutralizing antisera after immunization of rabbits, whereas unstructured recombinant VacA failed to induce a neutralizing response (Manetti et al., 1995). The high titre neutralizing antisera was shown to recognize primarily conformational epitopes, suggesting that the oligomeric structure is required for toxin activity and may be important for successful vaccination.

Here we report that purified active cytotoxin viewed in the transmission electron microscope revealed ordered hexameric and heptameric ring structures. Within each monomer two substructures could be observed that may represent the 37- and 58-kD subunits. Support for this hypothesis came from examination of preparations in which >90% of the 95-kD monomers had been cleaved into the 37- and 58-kD fragments. Toxin molecules from these highly processed preparations that had lost one of the visible subunits were observed. The structure is reminiscent of the structure of other bacterial toxins of the AB type in which enzymatic and membrane interaction functions are contained in different subunits and oligomerization is required for target cell interaction. We propose that the *H. pylori* toxin may belong to the AB family of bacterial toxins and may have evolved a similar strategy for interaction with the membrane of the target cell.

Materials and Methods

Purified Cytotoxin

Active cytotoxin was purified from the supernate of cultures of *H. pylori* strain CCUG17874 as previously described (Manetti et al., 1995). Purified active toxin was stored in PBS at 4°C for prolonged periods without loss of activity; however, the 95 kD underwent proteolytic cleavage that was complete after variable times between 15 d to 1 mo. Analytical gel filtration was performed in a SMART (Pharmacia, Uppsala, Sweden) system using a column containing Superose 6 (Pharmacia). 200-μl samples of toxin protein at a concentration between 80 and 120 μg/ml were loaded in each analysis. The column was calibrated using dextran blue (mol wt 2,000,000), thyroglobulin (mol wt 669,000), and catalase (mol wt 232,000) as molecular weight standards (Pharmacia). SDS-PAGE and immunoblot analysis were performed as described (Manetti et al., 1995) using rabbit antisera raised against recombinant fragments of the cytotoxin expressed in *Escherichia coli* (Telford et al., 1994*b*). Formaldehyde fixation was performed by incubating the toxin (200 μg/ml) in a solution of 25 mM lysine, 0.01% Thimerosol (Sigma Chemical Co., St. Louis, MO), and 0.01% formaldehyde in PBS for 48 h at 37°C and then dialyzing extensively against PBS.

Quick Freeze, Deep Etching, and EM

VacA molecules were prepared for microscopy by a procedure of absorption to mica followed by freeze drying (Heuser, 1983, 1989). Briefly, two drops of a suspension of finely ground mica flakes were added to 0.5 ml of a solution containing 10–30 μg purified toxin in PBS, and the toxin was allowed to adsorb to the mica for 30 s. The mica flakes were then pelleted by gentle centrifugation, washed twice with a solution of 70 mM KCl, 30 mM Hepes, pH 7.2, 5 mM $MgCl_2$, and layered onto a thin slice of aldehyde-fixed lung for support during freezing. This was accomplished by slamming the samples onto the liquid helium-cooled copper block of a quick freezing device (Cryopress; Med-Vac, Inc., St. Louis, MO).

Frozen mica flakes were freeze fractured in a freeze etching unit (Baf 301; Balzers S.p.A., Milan, Italy) and etched for 4.5 min at −104°C. Molecules absorbed to the mica were rotary replicated with ~2 nm of platinum applied from an angle of 10° above the horizontal and then backed with 25-nm-thick film of pure carbon. Replicas were separated from the mica by immersion in concentrated hydrofluoric acid and then picked up on 75-mesh formvac-coated microscope grids. Replicas were viewed in a transmission electron microscope (CM10; Philips Electronic Instruments, Inc., Mahwah, NJ) operating at 80 kV, and stereo images were obtained using ±10° of tilt with a eucentric side-entry goniometer stage.

Image Processing

Untilted micrographs (35K magnification) were digitized by a camera (XC77*e*; Sony, Montvale, NJ) mounted on a zoom microscope and connected to a Matrox IP8 frame grabber (Mesa, AZ). Micrographs were placed on a translation stage controlled by a personal computer. Contiguous frames were pasted together to produce image arrays of each negative of ~3,200 × 2,800 pixels (Lanzavecchia et al., 1994). Collages and further processing were carried out on a computer (355 Risc; IBM Corp., Danbury, CT).

Preliminary inspection of the images revealed four main types of quaternary structure. Individual molecules were selected and collected in galleries of homologous items. A total of 1,086 images (64 × 64 or 128 × 128 pixels) were processed for image averaging using the software package POLCA (Bellon and Lanzavechia, 1990). Groups of 30–100 molecules from a single negative were oriented and aligned to a reference chosen from the group to obtain an average. The average obtained was then used as a new reference to iterate the alignment. The process was repeated until no changes occurred. The results did not vary when different images were used as the first reference and were equivalent between different groups of homologous molecules. Mutivariate statistical analysis and hierarchical ascendant classification (Benzécri, 1992) of a group of 500 images, oriented according to a common reference, confirmed the visual classification into four groups. A few molecules whose automatic classification differed from visual classification or that gave origin to small isolated clusters were discarded from the averages.

Results

The molecular mass of the vacuolating cytotoxin in *H. pylori* culture supernatants has been estimated to be >600 kD (Manetti et al., 1995). High precision analytical gel filtration confirmed this molecular weight estimate (Fig. 1 *A*). Coomassie blue staining of this material after denaturing PAGE revealed a single 95-kD polypeptide (Fig. 1 *C*, lane *1*). In this preparation, trace quantities of the 37- and 58-kD products of proteolysis could be detected by immunoblot-

ting using antisera raised against recombinant VacA expressed in *E. coli* (Telford et al., 1994*b*) (Fig. 1 *D*, lane *1*). Upon aging in solution at 4°C, the purified toxin undergoes further processing until, after 15–30 d, most of the protein is cleaved into the 37- and 58-kD subunits (Fig. 1, *C* and *D*, lanes *2*). It is not clear if this processing is due to autoproteolysis or if the preparations were contaminated with trace quantities of proteases. The two subunits, however, appear to remain associated since the elution profile in analytical gel filtration is unaltered (Fig. 1 *B*). Fig. 2 *A* shows a representative field from electron micrographs after quick freeze, deep etching, and rotary replication of the intact material shown in Fig. 1 *A*. The majority of the protein is arranged in highly ordered structures showing six- or sevenfold symmetry. From the molecular weight estimates and the electrophoretic analysis, the simplest interpretation of these data is that the native toxin is formed of hexamers or heptamers of the 95-kD VacA polypeptide. In a selection of samples of different fields photographed in the EM, 70% of the recognizable structures were heptameric and 30% were hexameric. Approximately 10–15% of the molecules were not classifiable (Table I).

At higher magnification (Fig. 3, *A* and *B*), each monomer of the heptamer or hexamer structure is clearly resolved in two parts, a large lobe resembling a flower petal and a ring structure toward the center of the molecule. The overall diameter of the structure is ~30 nm, and the central ring cavity is ~12 nm. An immediate interpretation of this arrangement is that the two parts of the monomer visible in the molecule may represent the 37- and 58-kD subunits identified by the specific proteolysis of the 95-kD polypeptide after release from the bacteria (Telford et al., 1994*b*).

Support for this interpretation comes from the analysis of a highly purified preparation of toxin that was allowed to undergo proteolysis by prolonged storage at 4°C. Immunoblot analysis of this material revealed that ~90% of the 95-kD monomer had undergone proteolysis (Fig. 1 *C*, lane *2*). EM of this material revealed two distinct forms of the hexameric and heptameric structures (Fig. 2 *B*). One form was indistinguishable from the structures seen in unprocessed toxin, while the other resembled hexamers or heptamers of teardrop-shaped molecules in contact at their proximal ends (*arrows* in Fig. 2 *B* and shown at higher magnification in Fig. 3, *C* and *D*). These molecules appeared flatter than the molecules seen in the unprocessed material when three-dimensionality was viewed using stereo pairs of images taken at angles of −10° and +10° of tilt (Fig. 4).

Our interpretation of these images is that, upon cleavage of the 95-kD monomers in the oligomeric structures, the subunits forming the central ring can be dissociated to reveal the base of the molecule formed of the rod-shaped subunits. Since the processed subunits copurify in gel filtration with the intact molecules, and there was no obvious difference in the analytical gel filtration pattern between

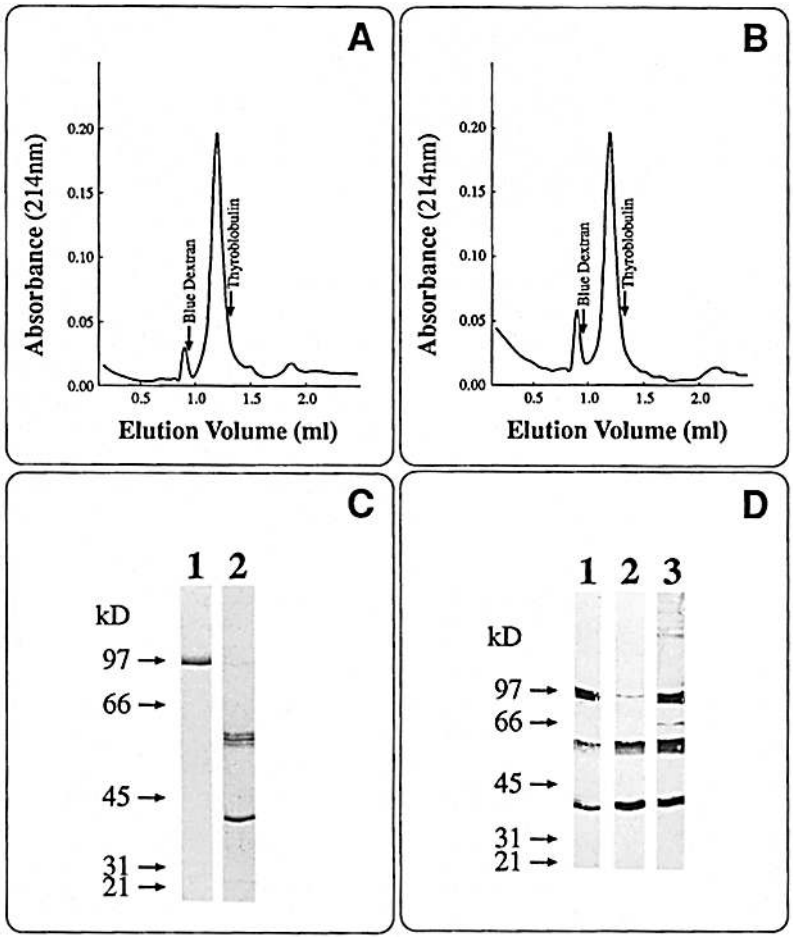

Figure 1. Analytical gel filtration of purified *H. pylori* cytotoxin. Superose 6 chromatography in a SMART system of freshly purified cytotoxin (*A*) and cytotoxin after prolonged storage at 4°C (*B*). The position of molecular weight standards (dextran blue, 2,000 kD; thyroglobulin, 669 kD) used to calibrate the column is shown. (*C*) Coomassie blue–stained SDS-PAGE of the preparations of toxin shown in *A* (lane *1*) and *B* (lane *2*). (*D*) Immunoblot of the material shown in *C* (lanes *1* and *2*) and the processed toxin after mild formaldehyde treatment (lane *3*). The position of molecular weight standards used in the electrophoresis is shown.

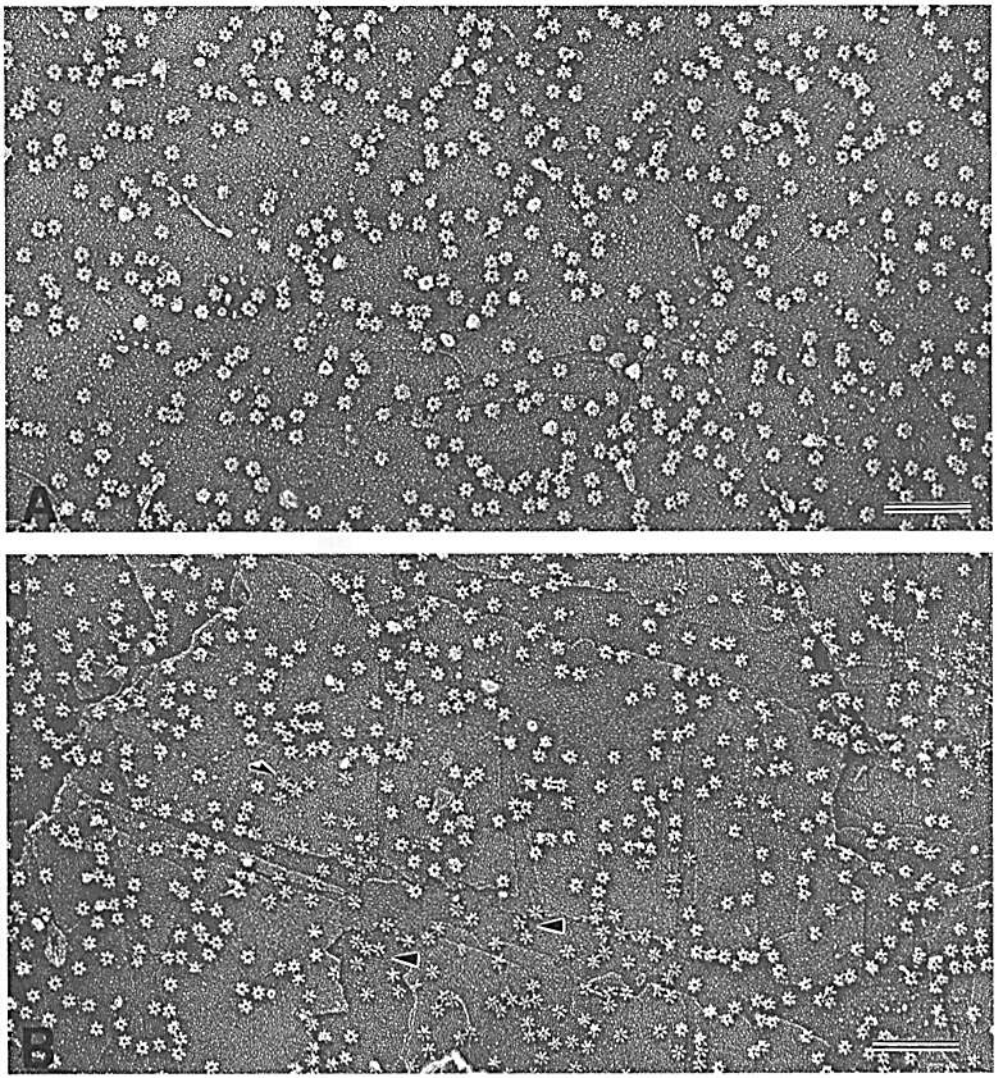

Figure 2. Transmission electron microscope visualization of purified toxin after quick freeze, deep etch preparation. (*A*) A representative field showing a large number of molecules from the unprocessed preparation of toxin shown in Fig. 1 *A*. (*B*) A similar sample of the proteolytically cleaved toxin shown in Fig. 1 *B*. The distribution of intact molecules and molecules that appear to have lost their central core (*arrows*) can clearly be observed. Bar, 200 nm.

the processed and unprocessed material (Fig. 1, *A* and *B*), we questioned whether the dissociation of the subunits was due to an artifact of sample preparation. To approach this question, the material shown in Figs. 1 *B* and 2 *B* that showed a high proportion of dissociated molecules was fixed by mild treatment with formaldehyde to stabilize the molecules without destroying the native structure (Rappuoli, 1994; unpublished observations). SDS-PAGE and immunoblotting of this material revealed a significant reduction in the proportion of 37- and 58-kD polypeptides with a corresponding increase in 95-kD and higher molecular weight material (Fig. 1 *D*, lane *3*), indicating that the formaldehyde treatment had, in part, fixed the two subunits together. EM of the same material revealed that >95% of the molecules retained the intact structure observed in the unprocessed preparation (Table I). Hence, the 37- and 58-kD subunits remain associated in the intact oligomeric structure after cleavage. In support of this interpretation, fixation of the processed toxin with fourfold higher concentration of formaldehyde resulted in quantitative conversion of the 58- and 37-kD subunits to the 95-kD monomer in the absence of significant intermolecular cross-linking (data not shown).

The dissociation of the central ring structure may have been caused by the charged environment close to the surface of the mica or by physical shearing of molecules sandwiched between two mica flakes during centrifugation. Either way, the flatter molecules were consistently observed in preparations of toxin that had undergone extensive cleavage of the 95-kD monomer into the 37- and 58-kD subunits, whereas they were rarely (<0.5%) observed in essentially intact preparations.

Table I. Distribution of the Different Cytotoxin Structures Observed

	Intact		Flat‡		
VacA preparation	7mer	6mer	7mer	6mer	Total (percentage flat)
A* (intact)	242	104	0	0	346 (0)
B (processed)	315	146	153	126	740 (38)
B (fixed)§	120	114	2	1	234 (1)

*A and B are the preparations of VacA shown in Fig. 2, *A* and *B*, respectively.
‡Flat refers to the structures observed in proteolytically cleaved preparations that appear less tall than the intact molecules (see Fig. 3, *C* and *D*).
§Proteolytically processed preparation shown in Fig. 2 *B* after mild fixing with formaldehyde.

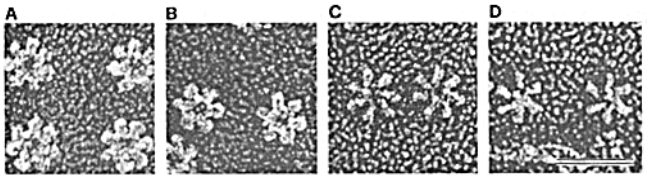

Figure 3. Higher magnification of the four forms of the toxin observed in Fig. 2, *A* and *B*. (*A*) Intact heptamers. (*B*) Intact hexamers. (*C*) Processed heptamers. (*D*) Processed hexamers. Bar, 50 nm.

The flatter molecules showing only the radial arms were only ~40% of the total, even if >90% of the monomers were cleaved into the 58- and 37-kD subunits. This may simply be a characteristic of the sample preparation. However, it may suggest that one or two uncleaved monomers are sufficient to keep the entire structure intact. In this case, 10% of intact 95-kD monomers would be sufficient to preserve the structure of 60–70% of the molecules.

The application of image clustering and averaging techniques (see Materials and Methods), made possible because of the rotary shadowing, has permitted a clearer visualization of the different structures observed. Fig. 5 *A* shows the result obtained by superimposition of a selection of molecules of each of the four forms observed. Approximately 100 molecules of each form were used to construct the images. In Fig. 5 *B*, each of these images was further subjected to rotational averaging. The images obtained by this analysis permit a better appreciation of the regularity and symmetry of the structures. Averaged images of all four groups display a propeller-like structure with a clearly appreciable handedness. The consistency in handedness indicates that the oligomers always attach to the mica on one face but not on the other, or else the opposite handedness would also be observed. Contour maps of the brightness of the averaged images (Fig. 5 *C*) suggest that the central subunits are rotationally displaced from the arms such that they overlap with the adjacent arm. Interaction of the central subunit of one monomer with the adjacent monomer may contribute to the stability of the oligomeric structure.

The relationship between the intact and processed molecules is more apparent in the averaged images. While the hexamers have a slightly smaller overall diameter than the heptamers, there is no significant difference in diameter between the processed and intact forms of the respective structures. A clear difference, however, can be observed in the outer extremity of the arms of the molecules between the intact and processed molecules. This may indicate that the presence of the central core of subunits in some way constrains the shape of the radial arms.

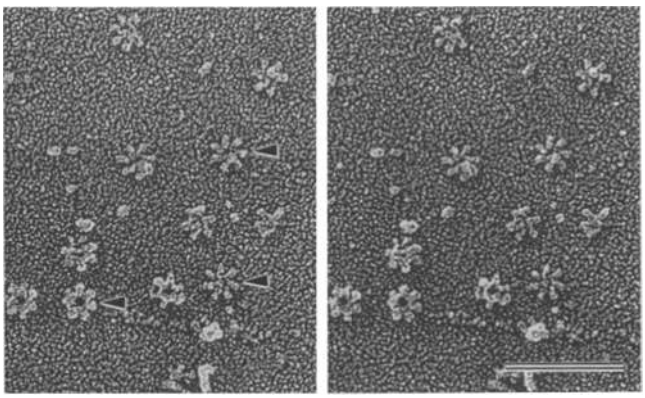

Figure 4. Stereo pairs of images of processed preparations of toxin taken at −10° and +10° of tilt. Bar, 100 nm.

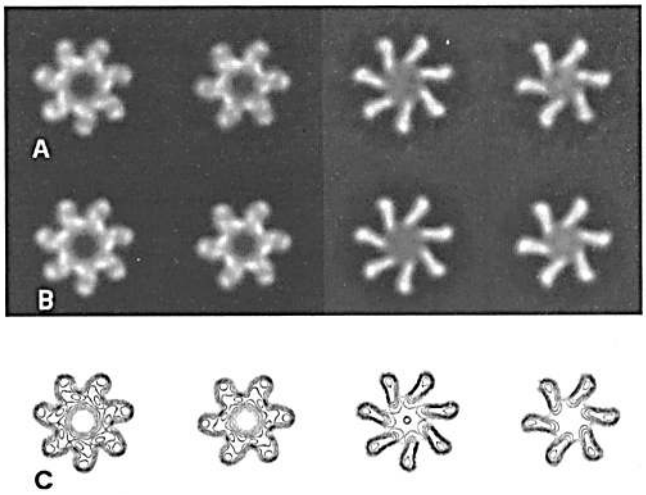

Figure 5. Image averaging of a selection of the different forms of the molecules seen in processed and unprocessed preparations of toxin. (*A*) Images formed by superimposition of ~100 individual molecules of each class. From left to right, the panels show intact heptamers, intact hexamers, processed heptamers, and processed hexamers. (*B*) Rotational averaging of the images shown in *A*. (*C*) Contour maps of the image intensity of the images shown in *B*.

Discussion

Our interpretation of the structure of the native toxin, based on the EM, is that the peripheral lobes and the central ring reveal structurally distinct subunits that are detected as 37- and 58-kD peptides in denaturing gel electrophoresis. The base and peripheral lobes of the molecule are formed by the interaction of one of the subunits that form the distorted cartwheel structure seen in proteolytically cleaved preparations. The second subunit can be observed as the central raised structure in the intact molecules. In the intact molecule, the small subunits are connected to the large subunits by a flexible loop of a repeat of eight hydrophilic amino acids (Telford et al., 1994*a*,*b*). Cleavage of this loop has no major effect on the overall structure in solution; however, fortuitous conditions of sample preparation resulted in removal of the central core of the molecule to reveal the base of the molecule formed by the large subunits. It may be that there is also interaction between the small subunits such that all monomers must be processed before the core can be lost. The consistent handedness observed indicates that only one face of the molecule interacts well with the mica.

Many bacterial toxins that act on intracellular targets are composed of two functionally distinct subunits. These di-chain or AB toxins contain an enzymatically active sub-

unit (A) whose translocation to the cytosol is dependent on interaction of the binding (B) subunit with the cell membrane (Montecucco et al., 1991). One common property of the isolated B subunits of these toxins is the capacity to interact with artificial or cellular membranes to form ion channels (Milne et al., 1994; Hoch et al., 1985). Membrane interaction is often dependent on low pH (Eriksen et al., 1994), suggesting that the toxins may be internalized by receptor-mediated endocytosis and may undergo a conformational change in the acidic environment of the endosome (Montecucco et al., 1991).

The structure of the *H. pylori* cytotoxin is reminiscent of the structure of these AB-type toxins. We have recently shown that the 58-kD subunit expressed in *E. coli* interacts irreversibly with artificial membranes at low pH and forms ion channels (Moll et al., 1995), which may indicate that the 58-kD subunit is analogous to the B moiety of di-chain toxins. This is consistent with the observation that the larger of the two subunits seen in the eletron microscope forms intramolecular interactions to form oligomers that can be observed in the absence of the small subunit. Furthermore, short exposure of the toxin at pH < 5.0 results in a dramatic increase in activity that is associated with altered circular dichroism and fluorescence properties consistent with the concept of acid-induced conformational changes (De Bernard et al., 1995).

Both intact and highly processed preparations of the toxin were active (data not shown), indicating that cleavage of the monomer does not inactivate the toxin. Based on the structural similarities with the di-chain toxins, it is tempting to speculate that cleavage of the loop between the subunits is necessary for the activity of the toxin. In this case, the preparations that are predominantly intact may be processed by target cell proteases as is the case for diphtheria (Collier, 1995) and cholera (Mekalanos et al., 1979) toxins.

The remarkable structural similarity in such diverse toxins may reflect a more general mechanism for membrane translocation of essentially hydrophilic macromolecules. Oligomerization may represent a convenient way of masking hydrophobic regions in a protein required for membrane interaction to ensure solubility in aqueous solution. Conformational changes on interaction with membranes could result in reversal of function such that hydrophobic patches become exposed to permit interaction with the membrane, and hydrophilic regions could form a channel through which an enzymatically active moiety could enter the cytosol.

If the analogy with AB-type toxins holds, then we might expect that the small 37-kD subunit should have enzymatic activity and should be translocated to the cytosol where it can act on its target substrate. The nature of the vacuolation in intoxicated cells has suggested that the toxin may interfere with late endosome structure or function (Telford et al., 1994*a*; Papini et al., 1994). Elucidation of the mechanism of action of the toxin may result in a parallel increase in the understanding of this stage of endocytosis, as the Clostridial toxins have contributed to the understanding of neuroexocytosis. Hence, the *H. pylori* cytotoxin may add to the powerful collection of bacterial protein toxins that serve as tools for the molecular dissection of intracellular processes in eukaryotic cells.

We thank P. Salvatici for expert technical assistance, and L. Gamberucci and G. Corsi for photography and artwork.

Received for publication 27 December 1995 and in revised form 21 February 1996.

References

Bahkdi, S., and J. Tranum-Jensen. 1991. Alpha-toxin of *Staphylococcus aureus*. *Microbiol. Rev.* 55:733–751.

Bahkdi, S., J. Tranum-Jensen, and A. Sziegolet. 1985. Mechanism of membrane damage by Streptolysin-O. *Infect. Immun.* 47:52–60.

Ballard, J., Y. Sokolov, W.-Y. Yuan, L. Kagan, and R.K. Tweten. 1993. Activation and mechanism of *Clostridium septicum* alpha toxin. *Mol. Microbiol.* 10: 627–634.

Bellon, P.L., and S. Lanzavechia. 1990. POLCA, a library running in a modern environment, implements a protocol for averaging randomly oriented images. *Comput. Appl. Biosci.* 6:271–277.

Benzécri, J.P. 1992. Correspondence Analysis Handbook. Marcel Dekker, Inc., New York. 665 pp.

Collier, R.J. 1995. Three-dimensional structure of Diphtheria toxin. *In* Bacterial Toxins and Virulence Factors in Disease. J. Moss, B. Iglewski, M. Vaughan, and A.T. Tu, editors. Marcel Dekker, Inc., New York. 81–93.

Cover, T.L., and M.J. Blaser. 1992*a*. Purification and characterization of the vacuolating toxin from *Helicobacter pylori*. *J. Biol. Chem.* 267:10570–10575.

Cover, T.L., and M.J. Blaser. 1992*b*. *Helicobacter pylori* and gastroduodenal disease. *Annu. Rev. Med.* 43:135–145.

Cover, T.L., M.K.R. Tummuru, P. Cao, S.A. Thompson, and M.J. Blaser. 1994. Divergence of genetic sequences for the vacuolating cytotoxin among *Helicobacter pylori* strains. *J. Biol. Chem.* 269:10566–10573.

De Bernard, M., E. Papinin, V. de Filippis, E. Gottardi, J.L. Telford, R. Manetti, A. Fontana, R. Rappuoli, and C. Montecucco. 1995. Low pH activates the vacuolating toxin of *Helicobacter pylori*, which becomes acid and pepsin resistant. *J. Biol. Chem.* 270:23937–23940.

Domenighini, M., M. Pizza, and R. Rappuoli. 1995. Bacterial ADP-ribosyltransferases. *In* Bacterial Toxins and Virulence Factors in Disease. J. Moss, B. Iglewski, M. Vaughan, and A.T. Tu, editors. Marcel Dekker, Inc., New York. 59–80.

Eriksen, S., S. Olsnes, K. Sandvig, and O. Sand. 1994. Diphtheria toxin at low pH depolarizes the membrane, increases the membrane conductance and induces a new type of ion channel in Vero cells. *EMBO (Eur. Mol. Biol. Organ.) J.* 13:4433–4439.

Harris, R.W., P.J. Sims, and R.K. Tweten. 1991. Kinetic aspects of the aggregation of *Clostridium perfringens* θ-toxin on erythrocyte membranes. *J. Biol. Chem.* 266:6936–6941.

Heuser, J.E. 1983. Procedure for freeze-drying molecules absorbed to mica flakes. *J. Mol. Biol.* 169:155–195.

Heuser, J.E. 1989. Protocol for 3-D visualization of molecules on mica via the quick-freeze, deep etch technique. *J. Electron Microsc. Tech.* 13:244–263.

Hoch, D.H., M. Romero-Mira, B.E. Ehrlich, A. Finkelstein, B.R. Dasgupta, and L.L. Simpson. 1985. Channels formed by botulinum, tetanus and diptheria toxins in planar lipid bilayers: relevance to translocation of proteins across membranes. *Proc. Natl. Acad. Sci. USA.* 82:1692–1696.

Lanzavecchia, S., P.L. Bellon, R. Dallai, and B.A. Afzelius. 1994. Three-dimensional reconstructions of accessory tubules observed in sperm axonemes of two insect species. *J. Struct. Biol.* 113:225–237.

Leppla, S.H. 1995. Anthrax toxins. *In* Bacterial Toxins and Virulence Factors in Disease. J. Moss, B. Iglewski, M. Vaughan, and A.T. Tu, editors. Marcel Dekker Inc., New York. 543–572.

Leunk, R.D. 1991. Production of a cytotoxin by Helicobacter pylori. *Rev. Infect. Dis.* 13 (Suppl.):686–689.

Manetti, R., P. Massari, D. Burroni, M. De Bernard, A. Marchini, R. Olivieri, E. Papini, C. Montecucco, R. Rappuoli, and J.L. Telford. 1995. The *Helicobacter pylori* cytotoxin: importance of native conformation for induction of neutralizing antibodies. *Infect. Immun.* 63:4476–4480.

Marchetti, M., B. Aricò, D. Burroni, N. Figura, R. Rappuoli, and P. Ghiara. 1995. *Helicobacter pylori* infection in a mouse model that mimics human disease. *Science (Wash. DC).* 267:1655–1658.

Mekalanos, J.J.R., R.J. Collier, and W.R. Romig. 1979. Enzymic activity of cholera toxin. II. Relationships to proteolytic processing, disulphide bond reduction and subunit composition. *J. Biol. Chem.* 254:5855–5861.

Milne, J.C., D. Furlong, P.C. Hanna, J.S. Wall, and R.J. Collier. 1994. Anthrax protective antigen forms oligomers during intoxication of mammalian cells. *J. Biol. Chem.* 269:20607–20612.

Moll, G., E. Papini, R. Colonna, D. Burroni, J.L. Telford, R. Rappuoli, and C. Montecucco. 1995. Lipid interaction of the 37 kDa and 58 kDa fragments of the *Helicobacter pylori* cytotoxin. *Eur. J. Biochem.* 234:947–952.

Montecucco, C., E. Papini, and G. Schiavo. 1991. Molecular models of toxin membrane translocation. *In* Sourcebook of Bacterial Protein Toxins. J.E. Alouf, and J.H. Freer, editors. Academic Press, New York. 45–56.

Papini, E., M. De Bernard, E. Milia, M. Bugnoli, M. Zerial, R. Rappuoli, and C. Montecucco. 1994. Cellular vacuoles induced by *Helicobacter pylori* originate from late endosomal compartments. *Proc. Natl. Acad. Sci. USA.* 91: 9720–9724.

Papini, E., E. Gottardi, E. Satin, M. De Bernard, J.L. Telford, P. Massari, R. Rappuoli, and C. Montecucco. 1995. Detection of V-ATPase on the membrane of intracellular vacuoles induced by VacA of *Helicobacter pylori*. *J. Med. Microbiol.* In press.

Parsonnet, J. 1993. *Helicobacter pylori* and gastric cancer. *Gastroenterol. Clin. North Am.* 22:89–104.

Rappuoli, R. 1994. Toxin inactivation and antigen stabilization: two different uses of formaldehyde. *Vaccine.* 12:579–581.

Schmitt, W., and R. Haas. 1994. Genetic analysis of the *Helicobacter pylori* vacuolating cytotoxin: structural similarities with the IgA protease type of exported protein. *Mol. Microbiol.* 12:307–319.

Sekiya, K., R. Satoh, H. Danbara, and Y. Futaesaku. 1993. A ring-shaped structure with a crown formed by streptolysin-O on the erythrocyte membrane. *J. Bacteriol.* 175:5953–5961.

Telford, J.L., A. Covacci, P. Ghiara, C. Montecucco, and R. Rappuoli. 1994*a*. Unravelling the pathogenic role of *Helicobacter pylori* in peptic ulcer: potential for new therapies and vaccines. *Trends Biotechnol.* 12:420–426.

Telford, J.L., P. Ghiara, M. Dell'Orco, M. Comanducci, D. Burroni, M. Bugnoli, M.F. Tecce, S. Censini, A. Covacci, Z. Xiang, et al. 1994*b*. Gene structure of the *Helicobacter pylori* cytotoxin and evidence of its key role in gastric disease. *J. Exp. Med.* 179:1653–1658.

van der Goot, F.G., J. Lakey, F. Pattus, C.M. Kay, O. Sorokine, A. Van Dorselaer, and J.T. Buckley. 1992. Spectroscopic study of the activation and oligomerization of the channel-forming toxin aerolysin: identification of the site of proteolytic activation. *Biochemistry.* 31:8566–8570.

Xiang, Z., S. Censini, P.F. Bayeli, J.L. Telford, N. Figura, R. Rappuoli, and A. Covacci. 1995. Analysis of expression of CagA and VacA virulence factors in 43 strains of *Helicobacter pylori* reveals that clinical isolates can be divided into two major types and that CagA is not necessary for expression of the vaculating cytotoxin. *Infect. Immun.* 63:94–98.

Zerial, M., and H. Stenmark. 1993. Rab GTPases in vesicular transport. *Curr. Opin. Cell Biol.* 5:613–620.